Proceedings of the Canadian Society for Mechanical Engineering International Congress
31st Annual Conference of the Computational Fluid Dynamics Society of Canada
CSME/CFD2024
May 26–29, 2024, Toronto, Ontario, Canada

SLOSHING PHENOMENON IN ARCHIMEDES SCREW PUMPS

Scott C. Simmons[1] and William David Lubitz[1*]
[1]School of Engineering, University of Guelph, Guelph, Canada
*wlubitz@uoguelph.ca

Abstract—Archimedes screw pumps are a fish-friendly pumping technology that are widely used for water pumping in land drainage and reclamation schemes, as well as in water and wastewater treatment facilities. Their design has room for improvement; and improved design could pump similar quantities of water with higher energetic (or economic) efficiencies. During an investigation of the effects of varying parameters on Archimedes screw performance, the authors noticed an undocumented flow phenomenon. In field studies of both screw pumps and Archimedes screw generators (hydropower orientation), variations in water level were noticed along the length of the screw. The variations were also present in laboratory experiments and numerical simulations. After further analysis, it was discovered that a periodic "sloshing" of water in the screw occurred during operation. The sloshing caused high-water points at consistent locations along the screw length. The sloshing seemed to be highly dependent on rotation speed and screw geometry.

Archimedes screw pump; computational fluid dynamics; water pumping; dynamic flow phenomena

I. INTRODUCTION

Archimedes screws are an ancient technology that have been primarily used for water pumping since antiquity [1]. The device is a helical array of blades wrapped around a central, cylindrical tube. In essence, the Archimedes screw is a more general form of an auger.

When used for water pumping, the Archimedes screw is usually housed in a fixed, cylindrical trough. For this purpose, the technology is usually referred to as an Archimedes screw pump (ASP). Figure 1 demonstrates this orientation alongside definitions of common design variables.

The trough must have a slightly larger diameter than the outer diameter of the screw blades (D_o) to prevent scraping and damage. The small difference in diameter leaves an intentional gap between the blades and the trough that has a designed gap width (G_w). Water that leaks through the gap is considered a loss and is termed "gap leakage" flow (Q_g).

Aspects of this work were financially supported by the Natural Sciences and Engineering Research Council (NSERC) Alliance Grants program (grant # ALLRP 561188 - 20) with Greenbug Energy Inc. (Delhi, ON, Canada).

The main design variables for ASPs are the outer diameter (D_o), inner diameter (D_i), pitch (S), flighted length (L), inclination angle (β), upper water level (h_U), lower water level (h_L), and rotation speed (ω). The screw outputs a flow rate (Q) of water that is primarily based on the geometry of the screw, lower water level, and rotation speed; though, since there are so many parameters to characterize a screw, it is difficult to accurately predict the output flow rate.

Another key variable used to describe an operating Archimedes screw is the bucket fill height ratio (f, often called "fill height"). The fill height ratio is used to describe the capacity of a screw, it is calculated as:

$$f = \frac{z_{wl} - z_{min}}{z_{max} - z_{min}} \tag{1}$$

where it is a function of the bucket water level (z_{wl}), and the minimum (z_{min}) and maximum bucket water levels (z_{max}). When the fill height ratio is $f = 1$, the buckets are at their maximum capacity before water overtops the inner diameter and spills into a lower bucket (called "overflow leakage", Q_o). Overflow occurs when $f > 1$.

ASPs are primarily used for pumping water in land drainage and reclamation schemes, as well as in water and wastewater treatment facilities. They have been used for land drainage in the

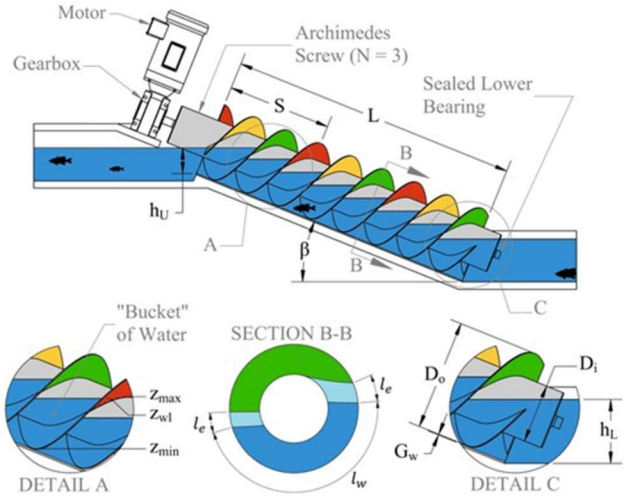

Figure 1: Archimedes screw pump layout with common variables. Detail views for bucket water levels (Detail A), wetted arc lengths for leakage analyses (Section B), and lower end of screw (Detail C).

Netherlands since the 1500s [2]; in fact, many traditional Dutch windmills operated wind-powered Archimedes screws to drain polders in lowland regions [3].

In a climate impacted future, the optimal design of land drainage technologies will be crucial. Research indicates that there are many improvements to be made to the design of Archimedes screw pumps.

Perhaps due to the historic nature of the technology, design of Archimedes screws seems to be primarily empirical in the English literature. It appears that many design guidelines in the literature are heuristic, either based on very old data or informed by generations of construction experience.

The most comprehensive document on ASPs is the Archimedian Screw Pump Handbook [3] (an updated version exists in the German literature [4]). The performance predicting models presented in the handbook are largely sourced from Muysken's journal article published in Dutch in 1932 [5]. The article comprehensively presents performance models that were informed by experimental results published earlier (1851 [6], 1916 [7], 1929 [8], and an unknown date [9]). Most of these papers could not be located, so it was difficult to ascertain the robustness or validity of the presented models; regardless, all the models were of an heuristic nature.

Muysken does present a model for predicting flow rate (Q) based on screw geometry and rotation speed:

$$Q = q \cdot \omega \cdot D_o^2 \qquad (2)$$

where q is a parameter derived from the free-surface geometry of a screw bucket. Some preliminary investigation parallel to this paper's study has suggested that Muysken's flow rate prediction can be accurate when subject to specific operating conditions, but it exhibits a higher degree of error in wider operating ranges. Muysken does identify the limitations in the flow rate model. Namely, it does not account for the impacts of overfilling buckets (manifested as "overflow leakage", Q_o), gap leakage (Q_l), friction effects, and the lower water level (h_L) conditions. With modern numerical methods and computational techniques, these phenomena may be more appropriately quantified.

Recent investigations into Archimedes screws have observed phenomena that may be more readily quantified with modern techniques [10, 11]. The authors have observed an event called the "sloshing phenomenon" in both Archimedes screw generators (ASGs) and pumps. The phenomenon was mentioned in a previous field study on ASGs [12], though it was not investigated further nor quantified.

The sloshing phenomenon occurred during screw operation. It appeared to be initiated by the in-rush of water at the screw's inlet. As water surged into the open screw bucket, it began to oscillate back-and-forth ("slosh") as the bucket translated along the screw's length. It was first observed by the authors in the laboratory. During laboratory experiments on ASGs [13], the bucket fill height (f) appeared to be consistently higher near the midpoint of the screw's length during operation. At the time, it was hypothesized that the phenomenon was an artifact of manufacturing imperfections (i.e., varying gap widths, etc.). However, high fill height levels were also observed near consistent points along the length of multiple full-scale ASG

Figure 2: the "sloshing phenomenon" was observed and noted in a field study the author's conducted on an Archimedes screw generator powerplant in Totnes, United Kingdom.

powerplants during the 2020 field study [12], including the powerplant in Totnes, United Kingdom (Figure 2).

A video was recorded at Totnes where the camera followed one bucket as it traversed the screw from inlet to outlet. It was observed that the free surface in the screw bucket would rise to one side while sinking on the other, then reverse that pattern from start to finish (i.e., it would slosh back and forth from start to finish). One consistent high point appeared to be near the midpoint of the screw and corresponded to the previously observed high bucket levels.

Interestingly, the sloshing phenomenon was also observed in numerical simulations of screw pumps. To address inaccuracies in performance models, the authors developed a computational fluid dynamic (CFD) model of an Archimedes screw pump. The model was run under a wide range of screw parameters (scale size, inclination angle, rotation speed, etc.). During the preliminary analysis of a simulation set, consistent, varying bucket fill heights were observed. When a single bucket was tracked along the screw's length, the sloshing phenomenon was observed in the CFD results.

Bucket water levels are key indicators of the sloshing phenomenon; however, to quantify sloshing, the water levels of both sides of the screw must be known. This is problematic for laboratory and field measurements; due to screw geometry, it is difficult to measure fill height on both sides of the buckets. The side of the bucket closer to the upper end of the screw (the "back") being harder to measure than the bucket side closer to the lower end (the "front") of the screw (cf. Figure 3). This was

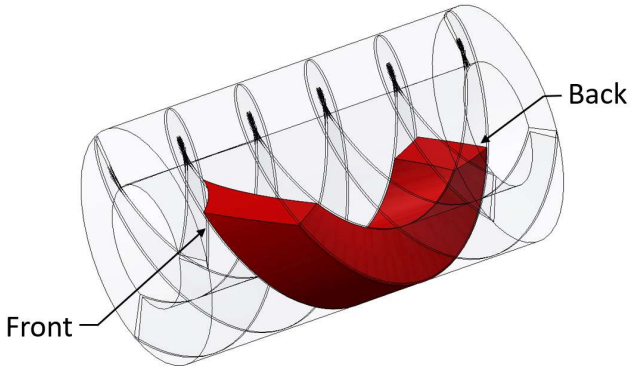

Figure 3: the back and front sides of a screw bucket within the domain

addressed by using a CFD model to simulate screw pump performance. The simulations were post processed to quantify the fill height on both the low-end and upper-end side of each bucket along the length of an operating screw. As a note: Section B in Figure 1 demonstrates the bucket water levels when viewing the screw normal to the axis of rotation. The higher water level corresponds to the "front" side of the bucket.

An investigation of the sloshing phenomenon has yet to be presented in the literature, perhaps because it is a dynamic flow phenomenon in a system that is largely impacted by static pressure-driven flow patterns. In any case, sloshing may have performance implications. It likely is an artifact of frictional effects, and a contributor to friction-driven power loss. It may also impact the torque-conversion capabilities of Archimedes screws. Sloshing does seem to be ubiquitous in operating screws: it has been observed in laboratory-scale screws, full-scale pumping stations, and in numerical simulations. Additionally, it was observed in both Archimedes screw generators and Archimedes screw pumps. So, this study will serve as an initial characterization of sloshing by investigating the impacts that a small variety of Archimedes screw pump operating conditions have on the phenomenon.

II. Methodology

A CFD model of a screw pump was developed to characterize sloshing. The details of the design, evaluation, and simulation sets used for the study are outlined in this section.

A. Numerical Model Design

Archimedes screw pumps exhibits a geometrically complex, unsteady, turbulent, free surface flow. To best approximate the complex flow system, the incompressible Reynolds-averaged Navier-Stokes (RANS) system of equations was solved using Menter's Shear Stress Transport (k-ω SST) [14] for turbulence closure. Flow was governed by the continuity equation and the RANS equations with a Boussinesq eddy viscosity assumption.

Menter's Shear Stress Transport turbulence model was selected since it seemed to approximate appropriate results when simulating Archimedes screw generators [15]. The model is also commonly used to approximate two-phase immiscible flow in hydraulic machinery [16]. The model combines and blends the k-ϵ and k-ω models to make use of the higher-accuracy conditions of both models. As such, the Shear Stress Transport model performs best when values of y^+ were kept either at $y^+ \leq 2$ or $y^+ \geq 30$.

The models were solved in OpenFOAM 8 [17]. An Euler scheme was used to discretize time, and an adaptive time step was used to improve performance. The solution algorithm iterated at each time step until it reached an appropriate condition (i.e., a Courant-Friedrichs-Lew number of $Co \leq 1$).

Second order central schemes were used to discretize gradient and Laplacian terms, and the divergence of velocity was discretized using a second order upwind scheme.

OpenFOAM's *interFoam* solver was implemented in the numerical simulations. The *interFoam* solver is used to solve two-phase, immiscible, incompressible flow systems. It uses the PIMPLE algorithm and the volume of fluid (VoF) method to resolve the system of equations. The PIMPLE algorithm is a combination of the PISO (Pressure Implicit with Splitting of Operator) and SIMPLE (Semi-Implicit Method for Pressure-Linked Equations) algorithms. The PIMPLE algorithm resolves transient systems by solving for steady conditions at an individual timestep, then incrementing time.

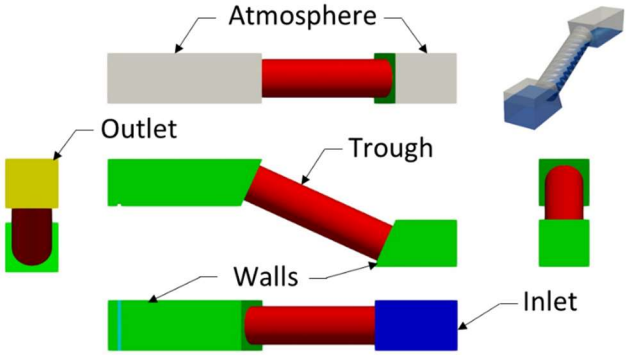

Figure 4: OpenFOAM simulation domain. Boundaries highlighted with colour: trough (red), atmosphere (white), walls (green), inlet (blue), and outlet (yellow).

The simulation domain and boundaries are shown in Figure 4. It was designed such that the simulated screw pumped water between a lower and upper basin. The bottom of the lower basin was set as a pressure-based water inlet. Water upwelled at the boundary to mitigate some impacts of boundary-induced flows. The screw was modelled within the trough boundary with a dynamic mesh. Arbitrary mesh interfaces (AMIs) were used to interface the rotating, dynamic mesh component to the statically meshed upper and lower basins. Water passed from the lower basin to the upper basin via the dynamically meshed, rotating screw. The upper basin had a small weir to control water levels. Water passed over the weir and into the pressure-based outlet boundary (set to atmospheric pressure). The tops of both basins were defined as atmospheric boundaries to vent any pressure buildup in the air-phase due to system flows.

B. Mesh Sensitivity Analysis

To ensure results were mesh-independent, five different mesh refinement levels were simulated over the same conditions (Figure 5).

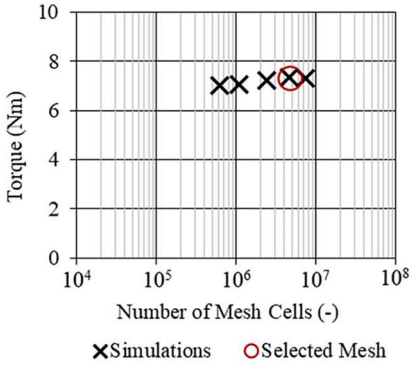

Figure 5: Mesh sensitivity analysis - selected mesh is highlighted.

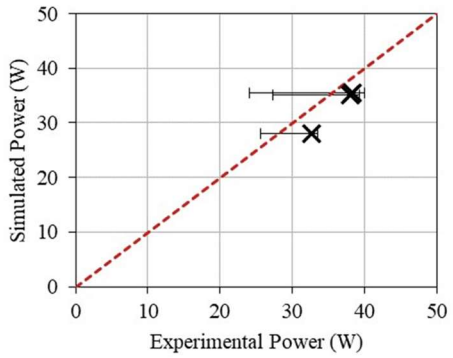

Figure 6: Model evaluation - a comparison between experimental data points and matching simulations. Screw geometry : Do = 0.316 m, Di = 0.168 m, S = 0.318 m, L = 1.219 m, N = 3, and beta = 26.3°. Data points varied in water levels and speed as documented in [10].

The results of the simulations indicated that the selected mesh would be appropriate to accurately approximate screw pump performance in the most computationally economic way.

C. Numerical Model Evaluation

The model was evaluated against three experimental data points. Experiments were run on a laboratory-scale screw pump [10]. Three representative points were taken from the collected data and simulations were modelled to match their operational conditions.

The output of the simulations seemed to agree within the uncertainty regions of the collected experimental data, which suggested that the CFD model was an accurate approximation of screw pump performance. Further, the screw pump CFD model was developed as an extension of the research group's Archimedes screw generator model which was shown to appropriate predict performance in screw generators that varied in size from small, laboratory-scale screws to the largest screw generator powerplant in the world (at time of publication) [15].

D. Simulations

To characterize the impacts of screw operation on sloshing, four simulations were run with different speeds. The geometry of the simulated screw was kept consistent for the four runs; it was modelled to match the laboratory screw in use when the phenomenon was first observed [10] (Table 1).

TABLE I. SIMULATION DETAILS

Run	Screw Parameters						
	ω (RPM)	D_o (m)	D_i (m)	S (m)	L (m)	N (-)	β (°)
1	10	0.316	0.168	0.318	1.219	3	24.5
2	20	0.316	0.168	0.318	1.219	3	24.5
3	40	0.316	0.168	0.318	1.219	3	24.5
4	60	0.316	0.168	0.318	1.219	3	24.5

Simulations were run until the screw reached a condition of regularly oscillating torque values, termed "quasi-steady state". Due to screw geometry, torque oscillated with the emptying and filling of the buckets. Simulations converged when torque oscillations were regular and repeating. At least 5 seconds of time was simulated under quasi-steady state conditions to capture multiple torque oscillations. Results were then time-averaged to find a characteristic representation of performance.

III. RESULTS AND ANALYSIS

Simulations were run according to Table 1. Results were compared along the length and inline to the axis of rotation of the screw. Data in this form may help observe patterns in bucket heights that indicate waveforms. Dimensional analysis was conducted to analyze results and allow for more direct comparisons to future simulations on a broader range of screws (i.e., varying size, inclinations, etc.).

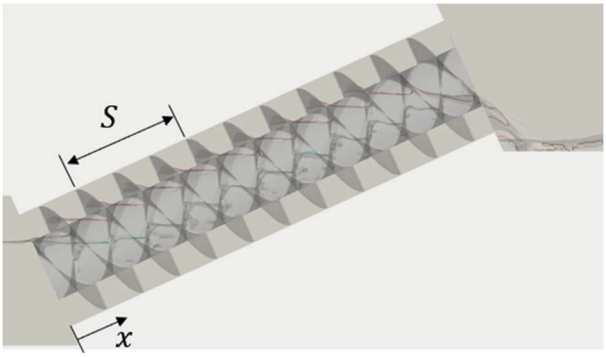

Figure 7: results of the 60 RPM simulation. The front bucket water levels are highlighted red and the back bucket water levles are highlighted blue. Parameters used to describe length along the screw (x) and pitch are also displayed.

In OpenFOAM, results were processed in run-time functions and redundantly measured in Paraview (OpenFOAM's native post processing graphical interface). In both cases, the location of the interface between water and air (water level) was measured as well as the minimum and maximum levels (z_{min} and z_{max}) associated with each bucket. Equation 1 was then used to show the results as the dimensionless bucket fill height ratio. These results are shown in Figure 8.

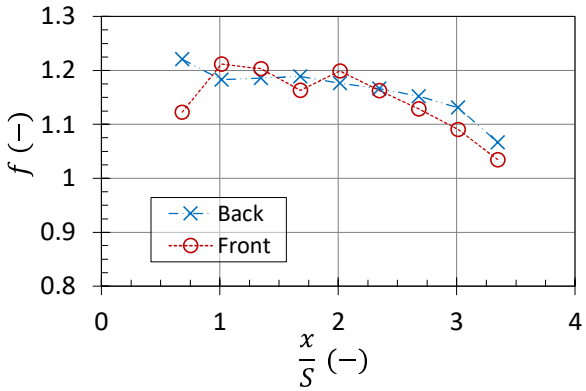

Figure 8: dimensionless fill height of the front and back side of the screw buckets along the dimensionless length of the screw.

To make the results in Figure 8 more broadly applicable, the length along the screw (x-axis) was given in a dimensionless form; the length along the screw, x, divided by the screw pitch, S (cf. Figure 7). In essence, the x-axis of Figure 8 is the number of pitch lengths (or screw turns) the bucket is positioned away from the inlet.

Figure 8 demonstrates the changes in the fill height at the front and the back of the bucket along the dimensionless length of the screw. The data shown in Figure 8 corresponds to the 60 RPM simulation case (i.e., "run 4"). Similar patterns were observed in the 10, 20, and 40 RPM cases as well. However, the 60 RPM case exhibited higher swings in amplitude, so the results were more easily observed and easy to distinguish.

The results in Figure 8 suggested that the sloshing phenomenon was occurring. It was evident since the fill height oscillations from the front to the back of the screw bucket seemed to mirror each other. When the front bucket increased in height, the back bucket correspondingly decreased, and vice versa. The trend was observed along the entire length of the screw, and it appeared that the amplitudes may be decreasing as the buckets approached the outlet. If that were the case, it would indicate that the sloshing was dampening along the length of the screw. However, it would be better to simulate a much longer screw (i.e., 20 or more buckets) before drawing a conclusion about this observation since a longer screw would allow for more sloshing and more time that the bucket is translating within the screw.

To better observe changes in amplitude of the simulation sets, the data was manipulated to compare it to the time that the bucket has been translating within the screw. A common parameter used to describe the translation of a screw bucket is the transport velocity. The transport velocity is shown in Equation 3:

$$v_T = \frac{\omega S}{60} \tag{3}$$

where rotation speed (ω) is in rotations per minute and the pitch is in metres.

Equation 4 was then used to convert the length along the screw (x) to the duration of time that the bucket has been within the screw (t).

$$t = \frac{x}{v_T} \tag{4}$$

To make observations easier, the data was normalized to reflect the difference in height between the front and back of the buckets. To do this, the average fill height of the bucket was found:

$$\bar{f} = \frac{f_{front} + f_{back}}{2} \tag{5}$$

Then the fill height of the front bucket was subtracted by the average fill height to represent the difference in height of the front and back of the screw bucket throughout operation. Either the front or back fill height could be selected, but the front fill height was selected since it corresponded to the side of the screw that was observed in the field study and laboratory experiments. The results were then plotted on the top graph of Figure 9. The

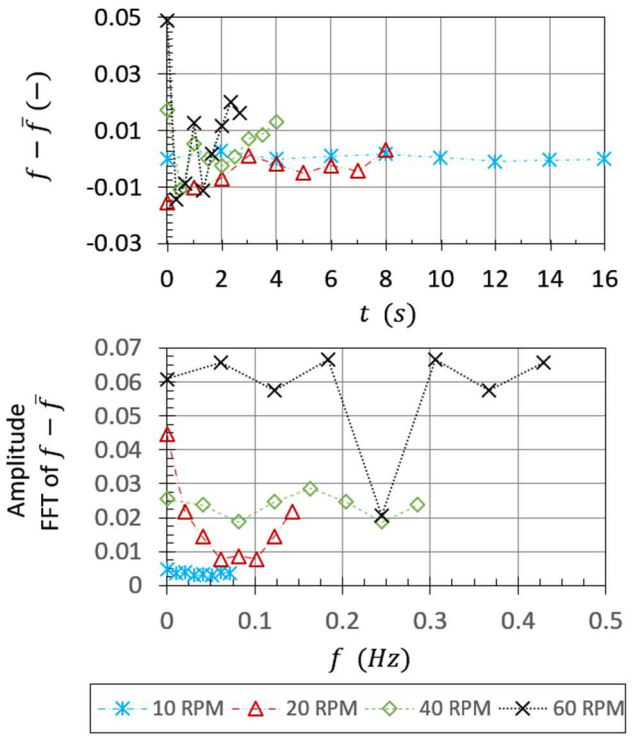

Figure 9: dimensionless fill height of the front and back side of the screw buckets along the dimensionless length of the screw.

graph shows the difference in the fill height from the fill height average against the duration of time that the bucket has been within the screw.

The results indicated that there may be predictable waveforms present within the dataset. Fast Fourier Transforms (FFT) were was taken of the time domain data. The results of the FFT are shown on the bottom graph of Figure 9. The bottom graph shows the amplitude of the FFT of the difference in fill height of the front bucket from the average fill height with respect to the sampling frequency.

The results suggest that waveforms were present in the data, and that they were impacted by changes in the rotation speed of the screw. The rotation speed seemed to impact both the amplitude and frequency of sloshing.

Sloshing in a real-world screw can be impacted by several factors (i.e., manufacturing defects that impact gap widths and blade shape, algae build-up causing variable surface roughness, etc.). In a numerical simulation, many external factors are removed since the simulation approximates performance in a "perfect" screw (i.e., a screw free of manufacturing imperfections, etc.). Therefore, the results shown in the figures demonstrate how sloshing is impacted strictly by the fluid mechanics in the system. The results suggest sloshing is impacted by dynamic effects related to rotation speed changes.

The sloshing seemed to first occur as water in-rushed to the first bucket at the screw's inlet; this was indicated by the high amplitudes of the first bucket / time zero data. The rotation speed seemed to impact the amplitude of the first bucket. As rotation speed increased, the amplitude of the first slosh increased. This

was likely due to the rotation direction and geometry of the screw's inlet (Figure 10).

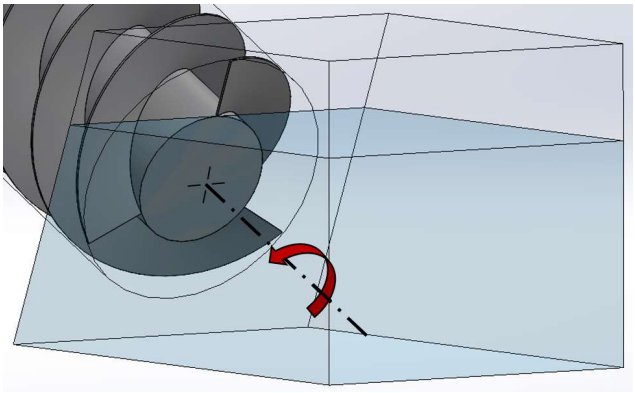

Figure 10: direction of rotation, shown at screw inlet (lower end).

As a screw pump turns, the blade end cuts downward through the free surface (the water-air interface) at, what will become, the back of the screw bucket. The blade motion continues with rotation, effectively pushing water into the bucket as the blade end cuts upward through the front side's free surface to close the bucket. Water rushed to the front side of the bucket during formation and sloshed to the back of the bucket during translation. The oscillations in fill height (the sloshing) continued throughout translation toward the outlet of the screw.

Changes in rotation also impacted wall shear stress. Wall shear impacts boundary layer flow and is directly related to friction. Friction at the screw blade walls could induce bucket sloshing in one direction and dampen it in the other. This may correspond to changes in amplitude throughout translation. However, it is suggested that further simulations on very long screws (i.e., screw with 20 buckets or more) could help observe the impacts of this phenomenon further.

IV. Conclusion

For the first time in the literature, fill height oscillations observed in operating Archimedes screws has been both documented and quantified. Fill height oscillations have been termed the sloshing phenomenon. Sloshing seemed to manifest as varying fill heights of screw buckets along the length of laboratory-scale screws, full-scale pumping station screws, and CFD screw simulations.

In this early analysis, the amplitude and frequency of sloshing was first quantified and presented in the results. It was observed that the rotation speed of the screw impacted both the amplitude and frequency of sloshing.

Sloshing may have implications on screw performance, though it has been suggested that screw performance is largely driven by static pressure gradients, so the impacts may be proportionally small. The authors suggest that further simulations varying both the scale size and proportional length of screw pumps should be conducted to investigate the phenomenon in more detail.

Acknowledgment

The authors gratefully acknowledge Tony Bouk and Brian Weber of Greenbug Energy Inc. (Delhi, Canada) for their continued help and support. The authors would also like to thank Chris Elliott of On Stream Energy Ltd. (Totnes, United Kingdom) for granting access, sharing data, and helping with surveying and measurements of screw generator installations – including the Totnes installation. The authors would also like to recognize the ongoing support of collaborator Guilhem Dellinger of the ICube laboratory's Mecaflu unit (Strasbourg, France).

References

[1] S. Dalley and J. P. Oleson, "Sennacherib, Archimedes, and the water screw: The context of invention in the ancient world," Technology and Culture, vol. 44, no. 1, pp. 1-26, January, 2003 2003, doi: https://www.jstor.org/stable/25148052.

[2] R. J. Hoeksema, Designed for Dry Feet: Flood Protection and Land Reclamation in the Netherlands. Reston: American Society of Civil Engineers, 2006.

[3] G. Nagel, Archimedian Screw Pump Handbook: Fundamental Aspects of the Design and Operation of Water Pumping Installations using Archimedian Screw Pumps. Schwäbisch Gmünd: RITZ-Pumpenfabrik OHG, 1968.

[4] G. Nagel and K.-A. Radlik, Wasserförderschnecken: Planung, Bau und Betrieb von Wasserhebeanlagen. Berlin: Pfriemer Buchverlag in der Bauverlag, 1988.

[5] J. Muysken, "Berekening van het nuttig effect van de vijzel," De Ingenieur, vol. 21, pp. 77-91, 1932.

[6] Storm and Buyzing, "Werktuig un Scheepsbow Modellversuche an Wasserförderschnecken," 1851.

[7] I. G. Horch, "Die Wasserförderschnecken," De Ingenieur, p. 945, 1916.

[8] H. Addison, "Experiments on an Archimedean Screw," The Institution of Civil Engineers: Selected Engineering Papers, vol. 75, 1929, doi: https://doi.org/10.1680/isenp.1929.14992.

[9] Hütte, "Drehzahlen an Schneckenförderern," ed. Berlin: Springer-Verlag.

[10] M. Lyons, S. C. Simmons, M. Fisher, J. S. Williams, and W. D. Lubitz, "Experimental Investigation of Archimedes Screw Pump," Journal of Hydraulic Engineering, vol. 146, no. 8, pp. 1–10, 2020, doi: https://doi.org/10.1061/(ASCE)HY.1943-7900.0001786.

[11] S. C. Simmons, L. Miller, M. F. Saudagar, C. Mendes, A. Yoosefdoost, and W. D. Lubitz, "An experimental study of Archimedes screw pump efficiency," presented at the Canadian Society for Mechanical Engineering International Congress 2023, Sherbrooke, 2023.

[12] S. C. Simmons, C. Elliott, M. Ford, A. Clayton, and W. D. Lubitz, "Archimedes screw generator powerplant assessment and field measurement campaign," Energy for Sustainable Development, vol. 61, April 2021 2021, doi: DOI: 10.1016/j.esd.2021.09.007.

[13] S. C. Simmons, K. J. Songin, and W. D. Lubitz, "Experimental investigation of the factors affecting Archimedes screw generator power output," presented at the Hydro 2017, Seville, 2017.

[14] F. R. Menter, "Two-equation eddy-viscosity turbulence models for engineering applications," AIAA Journal, vol. 32, no. 8, August 1994 1994, doi: https://arc.aiaa.org/doi/10.2514/3.12149.

[15] S. C. Simmons, "An experimental and numerical analysis of parameter scaling in Archimedes screw generators," PhD PhD Thesis, School of Engineering, University of Guelph, Guelph, 2021. [Online]. Available: https://atrium.lib.uoguelph.ca/server/api/core/bitstreams/7ef3ef6e-8fda-483c-9361-85910e083c18/content

[16] T. P. Dhakal and D. K. Walters, "Curvature and rotation sensitive variants of the K-Omega SST turbulence model," in ASME 2009 Fluids Engineering Division Summer Meeting, Vail, Colorado, 2010: ASME, doi: https://doi.org/10.1115/FEDSM2009-78397.

[17] OpenFOAM: Open Field Operation And Manipulation. ver. 8 openfoam.org: The OpenFOAM Foundation, 2020.